Strength and resource of the melting tool under thermomechanical loading

Konstantin A. Goncharov, Yury B. Chechulin

Abstract— High-purity titanium alloys are used to produce the most critical elements of aircraft structures. Refractory metals such as titanium, tungsten, molybdenum, niobium, zirconium are smelted in electron-beam furnaces. The melting point of these metals is much higher than the melting point of copper, this is the material, from which made melting tool. Therefore, a necessary condition for the smelting process is the forced cooling of the tool. Melting water-cooled tool is an essential structural component of vacuum-arc, plasma-arc and electron-beam furnaces, which are used to produce high-purity metals with high melting points. A characteristic feature of the design of the melting tool is limited resource. The paper is devoted to the calculation of the stress-strain state and the resource of a melting instrument under thermomechanical loading.

Keywords— Melting tool, stress-strain state, Navier-Stokes equations, heat transfer, mass transfer, electron-beam furnaces, nonlinear boundary value problem, finite element, low-cycle fatigue

I. INTRODUCTION

THE melting tool is subjected to thermal and mechanical loading during the smelting process of titanium alloy. As a result of such thermomechanical loading, irreversible plastic deformations appear in the melting tool. Plastic deformation changes the shape of the melting tool. Increasing the intensity of the deformation in the melting tool occurs with an increase in the number of heats [1]. Cracks appear and develop in areas of melting instrument where the value of the accumulated intensity of deformation exceeds the permissible value for material of the melting tool. As count of meltings does not exceed two thousand, so the investigating process of melting can be attributed to low-cycle fatigue [2,3]. The review of scientific publications has indicated, that data, which is used for low-cycle fatigue of metals, is dependent on type of laboratory tests, rate of cyclic loading , stress concentration, crack propagation, material property change and methods of analysis [4,5]. Currently, the number of mathematical models, which are used for prediction of the thermomechanical fatigue, is rather low. The uncertainties in the fatigue models are so high, that validating testing should always be performed, if it is possible. This is due to the complexity of providing of the experiments at high temperatures, the results of which are used in the mathematical model. In most engineering calculations it is advisable to use the theory of small elastoplastic strains. In this case, the stress and strain are calculated within a half cycle from the beginning of unloading, and the diagram of deformation in these coordinates can be approximated by various dependencies. With this approach it is possible to consider the deformation in each half cycle and to solve the elastic-plastic problem for this half-cycle. The hysteretic energy concept is conceivably a more rational basis for damage determination but the level of allowable hysteretic energy is difficult to define at present, and for complex structures it is not easily estimated. The analysis of stress-strain state and assessment of resource of the complex structure, such as a melting tool, were the main purpose of the study, results of which are given in the paper.

Manuscript received

K. A. Goncharov is with the Institute of Fundamental Education, Ural Federal University, Yekaterinburg, Russia, (phone: 343-375-4533; fax: 343-375-4533; e-mail: gonkonstant@yandex.ru).

Y. B. Chechulin is with Institute of Mechanics and Machine-Building, Ural Federal University, Yekaterinburg, Russia, (phone: 343-216-7117; fax: 343-216-7117; e-mail: uchechulin@mail.ru).

II. PROBLEM FORMULATION

In electron-beam furnace the heating of metal is performed by the transformation of the kinetic energy of the electron flux, which is moving directionally at high speed, into heat energy as a result of shock interaction with the metal surface.

Melting takes place in a sealed vacuum chamber with a maximum value of the pressure not exceeding 0,07 Pa. The source of free electrons is a special tungsten cathode, which is heated to high temperatures. After the departure from a heated tungsten cathode, the electrons enter in the electric field and accelerated by a potential difference between anode and cathode.

The melting tool is subject to thermomechanical loading in the process of melting of the ingot. Since the melting point of copper is much less, than the melting point of titanium alloy, the melting tool must be cooled during the melting process. For this purpose, the cooling channels were designed for the water flow in the melting tool. For efficient cooling it is necessary to solve the problem of heat transfer between the metal melt, melting tool and coolant. Insufficient water flow will cause it to boiling and turning into steam. On the contrary, excess consumption will be accompanied by intensive heat removal and, consequently, the heat loss during the melting process. It is necessary to solve the problem of heat conduction with sufficient exactness for a reliable analysis of the effectiveness of the melting tool's cooling system. The

solution to this problem allows us to determine the optimum flow rate of cooling liquid in the channel of the cooling system and temperature fields in the melting tool. The temperature distribution is required for reliable determination of the stress-strain state and a resource of the melting tool. This, in turn, is the main purpose of the performed study.

III EQUIPMENT DESCRIPTION

The cross section of electron-beam furnace is shown in the Fig. 1.

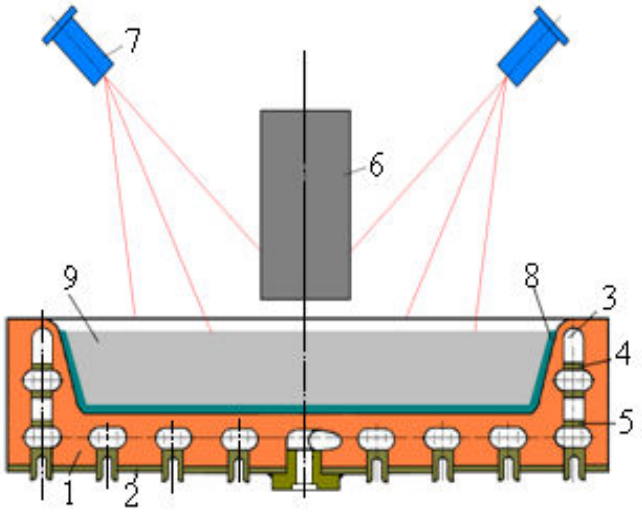

Fig.1 Cross section of electron-beam furnace: 1 plate, 2 – sheet of stainless steel, 3 – water flow channel, 4, 5 - partitions, 6 - cylindrical ingot, 7 - electron gun, 8 - skull; 9 - the molten metal (flat ingot).

Melting tool includes a housing structure, consisting of a bimetallic solid-rolled plate. The bimetallic plate, in turn, contains a copper plate 1 and a sheet of stainless steel 2, which are connected by means of explosive welding. A shaped groove 3 is made in the housing. This groove contains serially connected channels which are formed by means of the partitions 4 and 5. These channels are designed for a flow of coolant. Above the melting tool is melted ingot 6, which can be moved in the vertical direction by means of a special drive. The flow of electrons from the electron gun strikes the cylindrical surface of the ingot, and it is heated to the melting point.

The thin stream of molten metal flows along the ingot and falls down to the melting tool. Thermal conductivity of copper water-cooled tool is greater, than that of the melt, and therefore a layer of solidified melt with the thickness of 10...15 mm appears on its walls.

This layer is a kind of lining or a boundary layer called skull 8. To prevent solidification of the melt it is necessary to periodically emit electron flows from both guns to the surface of the melt in the melting tool. During the process of electron beam melting a spot with the diameter of about one centimeter moves over the surface of the liquid metal and performs a complex motion. This motion consists of rotation around the axis of symmetry and the discrete radial displacement perpendicular to the axis [6,7]. Such a periodic heating of the melt contributes to its distribution inside and filling of melting tool. Fig. 2 shows a cross section of the melting tool and its sizes.

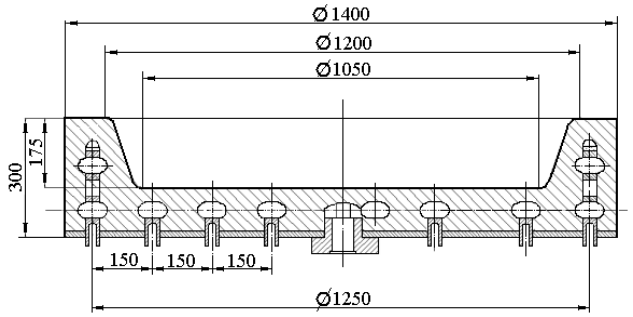

Fig.2 The geometry of the melting tool

The geometry of the melting tool let to produce a flat ingot weighing 800 kg.

IY DEVELOPMENT OF A MATHEMATICAL MODEL FOR CALCULATING TEMPERATURE FIELDS

Two time intervals are considered while solving the problem of filling the melting tool out with molten metal from the source cylindrical ingot. The first time interval is related to the duration of growth of the flat ingot inside the melting tool and takes up to three hours. The second depends on the electron beam scanning at the points of the melt surface and does not exceed one second.

Considering the facts marked above, differential equations that allow to take into account the size of the molten metal bath, were made for a time **t**, which characterizes melting process in a quasi-steady mode. This fact was taken into account while developing computational mathematical model. The process of forming flat ingot in the melting tool is a complex phenomenon of heat transfer at the free surface of liquid metal, which includes:

1. Direct supply of energy with directed electron stream;
2. Radiation from a free surface to the walls of the surrounding vacuum chamber;
3. Heat transfer by evaporation of metal and alloying elements;
4. Heat transfer through drops of molten metal from the ingot.

It was believed that the free surface is flat. This assumption was confirmed by visual observations during the regular heats. At the site of interaction of an electron beam with the melt, there may be some violations of the surface, this occurs due to evaporation and thermocapillar convection.

The basis for constructing a mathematical model is a classical system of three-dimensional Navier-Stokes equations for convection heat and mass transfer. It is derived from the general Navier-Stokes equations for a compressible fluid under the assumption, that the melt is dynamically and statically incompressible, ie, its density does not depend on pressure, but depends on temperature.

Differential equations for the transfer of momentum, mass and heat can be written as:

$$\frac{\partial \overline{V}}{\partial t} = -(\overline{V}\nabla)\cdot\overline{V} - \frac{1}{\rho}\nabla p + \nu\Delta\overline{V} + g\cdot\beta\cdot T;$$
$$div\overline{V} = 0; \quad (1)$$
$$\rho\cdot C_p\cdot[\frac{\partial T}{\partial t} + \overline{V}\cdot(\nabla)T] = \lambda\Delta T.$$

In this system, the quantities to be determined are the velocity vector

$$\overline{V} = \bar{i}\cdot Vx + \bar{j}\cdot Vy + \bar{k}\cdot Vz,$$

pressure **p**, temperature **T**. Both depend on the spatial coordinates and time. The parameters of equation (1) are the density **ρ**, kinematic viscosity ***ν***,thermal conductivity **λ**, specific heat at constant pressure $\mathbf{C_p}$, as well as gravitational acceleration **g** and the coefficient of thermal changes in the density **β.** In the projections on the axes of the spatial Cartesian coordinate system the Navier-Stokes equations have the form [8-12]:

$$\frac{\partial Vx}{\partial t} = -(Vx\cdot\frac{\partial Vx}{\partial x} + Vy\cdot\frac{\partial Vx}{\partial y} + Vz\cdot\frac{\partial Vx}{\partial z}) - \frac{1}{\rho}\cdot\frac{\partial p}{\partial x} +$$
$$+\nu\cdot(\frac{\partial^2 Vx}{\partial x^2} + \frac{\partial^2 Vx}{\partial y^2} + \frac{\partial^2 Vx}{\partial z^2});$$
$$\frac{\partial Vy}{\partial t} = -(Vx\cdot\frac{\partial Vy}{\partial x} + Vy\cdot\frac{\partial Vy}{\partial y} + Vz\cdot\frac{\partial Vy}{\partial z}) - \frac{1}{\rho}\cdot\frac{\partial p}{\partial y} +$$
$$+\nu\cdot(\frac{\partial^2 Vx}{\partial x^2} + \frac{\partial^2 Vy}{\partial y^2} + \frac{\partial^2 Vy}{\partial z^2}) + g\cdot\beta\cdot T; \quad (2)$$
$$\frac{\partial Vz}{\partial t} = -(Vx\cdot\frac{\partial Vz}{\partial x} + Vy\cdot\frac{\partial Vz}{\partial y} + Vz\cdot\frac{\partial Vz}{\partial z}) - \frac{1}{\rho}\cdot\frac{\partial p}{\partial z} +$$
$$+\nu\cdot(\frac{\partial^2 Vz}{\partial x^2} + \frac{\partial^2 Vz}{\partial y^2} + \frac{\partial^2 Vz}{\partial z^2});$$
$$\frac{\partial Vx}{\partial x} + \frac{\partial Vy}{\partial y} + \frac{\partial Vz}{\partial z} = 0$$
$$\frac{\partial T}{\partial t} = -(Vx\cdot\frac{\partial T}{\partial x} + Vy\cdot\frac{\partial T}{\partial y} + Vz\cdot\frac{\partial T}{\partial z}) +$$
$$+\frac{\lambda}{\rho\cdot C_\rho}\cdot(\frac{\partial^2 T}{\partial x^2} + \frac{\partial^2 T}{\partial y^2} + \frac{\partial^2 T}{\partial z^2});$$

The boundary conditions should be formulated to solve the system of equations (2). On the surface of skull each velocity component equals to zero:

$$Vx = Vy = Vz = 0$$

The expression for the surface tension as a function of temperature on the flat surface of the melt can be expressed as:

$$\sigma = \sigma_0 - \alpha\cdot(T - T_0),$$

to stress:

$$\overline{V} = 0,\ \mu\frac{\partial V}{\partial n} = \frac{\partial\sigma}{\partial l} = -\alpha\frac{\partial T}{\partial l}; \quad (3)$$

σ_0 = 7,2 H/m - surface tension at temperature T_0 = 20 °C; $\alpha \approx 0{,}26$ мН/(m·K) - temperature coefficient of surface tension, where n - normal, *l* - the tangent to the surface of the liquid, μ - dynamic viscosity of the melt [Pa · s].

At the free surface of the melt Neumann boundary conditions [13-15] are formed in the following way:

$$\lambda\frac{\partial T}{\partial n}\Big|_{\Omega} = q,\ \ q = \frac{P(r,t)}{A},$$
$$r = \sqrt{x^2 + y^2},\ A = \pi\cdot(r^2 - r_0^2(t)) \quad (4)$$

$r_0(t)$ - the radius of the scan at the current time t, R-radius of the melt at a depth h from the free surface; q-value of the intensity of the heat flux supplied to the melt surface Ω; A - surface area of the melt;
n-normal to the surface Ω; P (r, t) - power of the electron beam at the current time t.

$$P(r,t) = P_0\frac{\int_r^{r+\Delta r} e^{-\frac{(r-r_0(t))^2}{2\cdot\delta^2}}dr}{\int_0^R e^{-\frac{(r-r_0(t))^2}{2\cdot\delta^2}}dr}$$

P_0 = 300 kW - rated power of the electron gun,
δ - standard deviation of the radius of the scan.
The heat flux emitted from the free surface is determined by the Stefan-Boltzmann law

$$q_u = \varepsilon\cdot\sigma_c\cdot(T^4 - T_c^4) \quad (5)$$

where ε - the emissivity of the reduced system, consisting of a melting tool and a vacuum chamber, depending on its geometry and on the radiative properties of the free surface of a melting instrument and the inner surface of the chamber. In the following calculation we assumed, that ε = 0,49; σ_c - Stefan-Boltzmann constant,

$$\sigma_c = 5{,}67\cdot10^{-8}\frac{Bm}{м^2\cdot K^4};$$

T - temperature of the melt free surface and the outer surface of the melting tool,
Tc - temperature of the inner wall surface of the vacuum chamber.

The boundary conditions on the surface of the cooling channel can be formed as

$$Q = -C_B\cdot R\cdot(T - T_B), \quad (6)$$

where Q-value of the intensity of the heat flow exhaust with water, C_B - specific heat of water, R - consumption of water, T_B - the temperature of cooling water.

Resistance thermometers that record the water temperature in real-melting set at the inlet and outlet of the cooling system of the tool during the melting experimental melts. Analysis of the evidence of resistance thermometers showed that the temperature difference between inlet and outlet of melting tool, depending on the flow rate does not exceed 3,3 ... 6,8 °C. This allows us to conclude that the temperature of cooling water at all points of the cooling channels can be considered as a value equal to the average readings of resistance thermometers at the inlet and outlet.

During the calculation the thermophysical characteristics of the melt titanium alloy were chosen as follows:
The melting temperature Tm = 1670 °C,
Thermal conductivity λ = 22,5 W /(m · K)
Density $\rho = 4770$ kg/m^3,
The dynamic viscosity $\mu = 5{,}2 \cdot 10^{-3}$ Pa · s,
Specific heat capacity Cp = 540 J / (kg · K)
The linear expansion coefficient at 293 K was taken as
$\beta = 9{,}15 \cdot 10^{-6}$ 1 / K.

The thermophysical properties of copper in the temperature range 20 ... 250°C differ slightly, so their values were considered constant during the calculation of temperature fields of the melt and the melting tool for. The thermophysical properties of copper were taken as follows:
Density $\rho_c = 8950$ kg/m^3,
The specific heat Cc = 385 J / (kg ·K),
Coefficient of thermal conductivity λc = 390 W/(m·K)

Cooling water temperature was assumed to be $T_в$ = 30 °C. The number of guns was equal to two, their management was carried out by the developed program, which allows the electron beam impact on the free surface of the melt and the cylindrical surface of the molten ingot. The integration step was taken equal to 0,5 s. The computations with steps less than chosen above did not lead to a significant change in the results.

Y CALCULATION OF TEMPERATURE FIELDS

The system of equations (1) - (6) is performed by the numerical method of finite elements with using of the ten node solid finite element and with using of the software package ANSYS [16-21]. Dimensions of finite elements in the volume melt significantly different. Elements with the smallest sizes are located at the free surface of molten metal. Size of element increases with increasing of distance from this surface.

Fig. 3 shows a mosaic of temperature fields in molten titanium alloy at the final stages of melting. The only half of the ingot is shown on the figure to facilitate the analysis and perception of the information. This half was obtained by cutting the ingot with using the diametral plane of symmetry. Well-defined temperature range corresponds to each color shade. It can be seen that the areas, painted with the same color represent a body with shape similar to an ellipsoid of revolution. The bottom fragment of Fig.3 shows a graph describing the change of temperature on the melt free surface along the radius. It is seen, that the temperature of the melting free surface exceeds the melting point of titanium in the interval from 0 to 245 mm. Thus, the developed computational model based on numerical solution of differential equations of convective heat transfer, allows us to determine the temperature field and the profile of the metal bath.

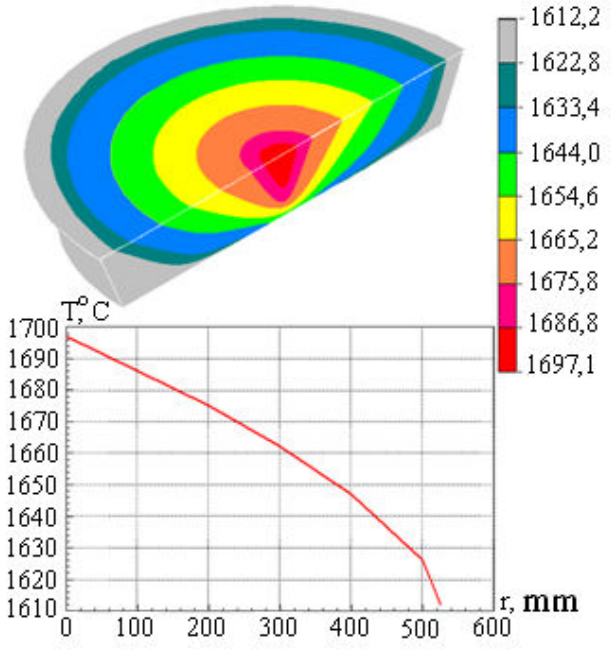

Fig.3 Mosaic of temperature fields in the melt

Two fragments, which are depicted in Fig. 4, characterize the temperature distribution in the melting tool at the final stages of melting.

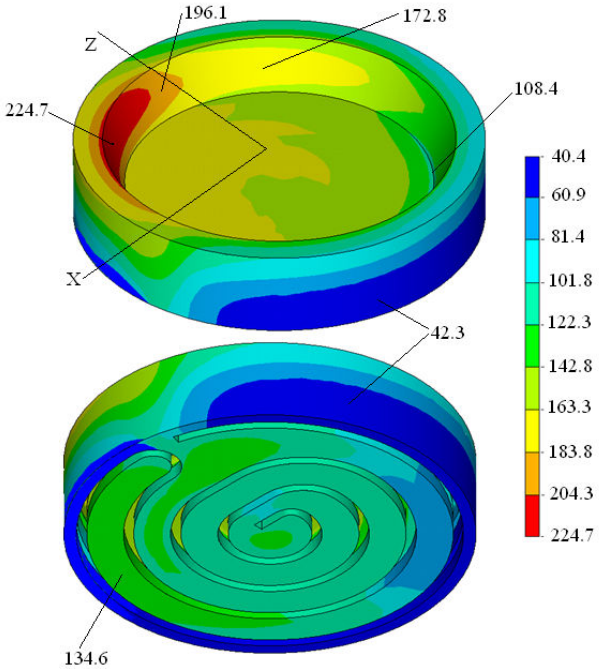

Fig.4 Mosaic of temperature fields in the melting tool, ° C.

An isometric view of the niche for the formation of a flat ingot of titanium alloy is shown in the upper fragment.The opposite lower portion, containing the cooling channels, is shown in the lower fragment.

The scale on the right side of Fig. 4 contains colors, which characterize the temperature ranges on the color mosaic. It is seen, that region of the highest temperatures, marked with red, is located on the inner side of the niche. The area of the highest temperatures is located on the conical surface of a niche, middle between the upper and lower edge. The maximum value of the temperature is equal to 224,7 ° C. This fact can be explained by the absence of the peripheral cooling channels in this area. In the field, painted with dark blue and located at the intersection of the lateral surface of the melting tool and it bottom plane, the value of temperature is the lowest. The interval of variation of these temperatures is in the range of 40 - 60,9° C.

The two curves, that characterize the temperature distribution along the perimeter of the board of the melting tool's niches, are shown in Fig.5 in the polar system of coordinates. The beginning of the polar coordinate system coincides with the axis X, shown in Fig. 4. Temperature scale is located on the vertical axis and contains the values of temperatures in the range from 110°C to 210°C, differing by 10°C. Curve 1 shows the temperature distribution on the circumference with a diameter of 1200 mm, which is the line of intersection of the inner conical surface and the upper ring surface of the melting tool. Curve 2 characterizes the temperature distribution around the circumference of a diameter of 1050 mm, which is the line of intersection of the inner conical surface and a bottom surface of the niche.

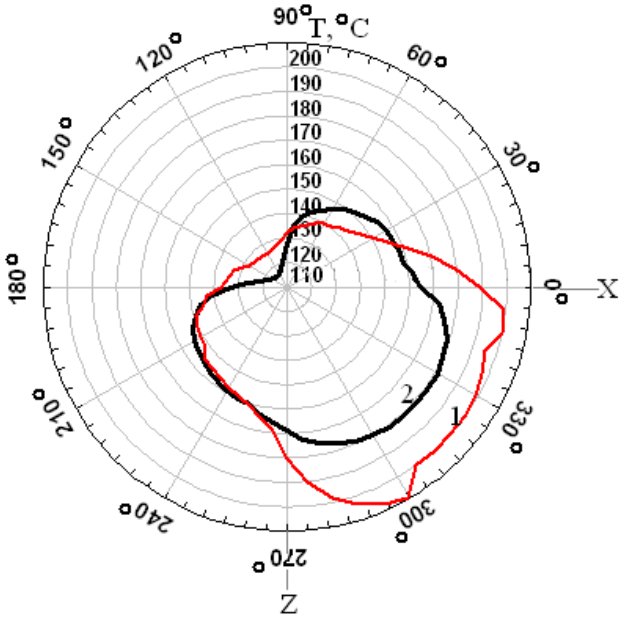

Fig.5. The temperature distribution along the perimeter of the board of the melting tool's niches

Analysis of the depicted curves indicates, that the difference in temperature between the upper and lower edge of the most heated inner surface of the niche has a place in the greater length of the circumference. The intersection of the curves indicates the equality of temperature on the edges of the conical surface of the niches. It is observed at certain points, which ate located at different angles. In addition, the curves are very close to each other on a small circumference, situated at an angle of 240°.

The temperature difference at different points in the melting tool leads to the appearing of temperature gradients in its design, which are accompanied by a thermal deformation.

YI CALCULATION OF THE STRESS-STRAIN STATE OF THE MELTING TOOL

In addition to the thermal strains, caused by temperature gradient, pressure, which transmitted to the bottom and wall of a niche from the weight of the melt, was also taken into account. The pressure was determined on the basis of the ratio

$$p = \rho \cdot g \cdot h, \qquad (7)$$

where ρ-density of melt, h – the height of the melt .

The relationships between normal stresses and the relative linear deformations can be written as [22]:

$$\begin{aligned} \sigma_x &= \frac{E}{1+\mu}\left(\varepsilon_x + \frac{3\mu}{1-2\mu}\varepsilon_m\right) \\ \sigma_y &= \frac{E}{1+\mu}\left(\varepsilon_y + \frac{3\mu}{1-2\mu}\varepsilon_m\right) \\ \sigma_z &= \frac{E}{1+\mu}\left(\varepsilon_z + \frac{3\mu}{1-2\mu}\varepsilon_m\right) \end{aligned} \qquad (8)$$

.

where $\varepsilon_m = \dfrac{\varepsilon_x + \varepsilon_y + \varepsilon_z}{3}$ - the average value of relative linear deformation, E- modulus of longitudinal elasticity of the tool's material , μ - the coefficient of transverse strain.

Similar relations between shearing stresses and angular deformations are of the form

$$\tau_{xy} = G\varepsilon_{xy},\ \tau_{xz} = G\varepsilon_{xz},\ \tau_{yz} = G\varepsilon_{yz} \qquad (9)$$

where $G = \dfrac{E}{2\cdot(1+\mu)}$ - modulus of transverse elasticity of the tool's material.

The intensity of stresses and intensity of strains is introduced in consideration with respect to the complex stress state

$$\sigma_i = \frac{\sqrt{2}}{2}\sqrt{(\sigma_x-\sigma_y)^2+(\sigma_x-\sigma_z)^2+(\sigma_y-\sigma_z)^2+6\cdot(\tau_{xy}^2+\tau_{xz}^2+\tau_{yz}^2)} \qquad (10)$$

$$\varepsilon_i = \frac{\sqrt{2}}{2(1+\mu)}\sqrt{(\varepsilon_x-\varepsilon_y)^2+(\varepsilon_x-\varepsilon_z)^2+(\varepsilon_y-\varepsilon_z)^2+\frac{3}{2}\cdot(\gamma_{xy}^2+\gamma_{xz}^2+\gamma_{yz}^2)}$$

The relationship between the intensity of the stress and the intensity of the strain determined in accordance with the generalized Hooke's law

$$\sigma_i = E\varepsilon_i \qquad (11)$$

The relationship between the deformations and the stresses under the simultaneous action of mechanical loads and the thermal loading of can be written as

$$\varepsilon_x = \frac{1}{E}[\sigma_x - \mu(\sigma_y + \sigma_z)] + \alpha \cdot \Delta T$$
$$\varepsilon_y = \frac{1}{E}[\sigma_y - \mu(\sigma_x + \sigma_z)] + \alpha \cdot \Delta T \quad (12)$$
$$\varepsilon_z = \frac{1}{E}[\sigma_z - \mu(\sigma_x + \sigma_y)] + \alpha \cdot \Delta T$$
$$\varepsilon_{xy} = \frac{\tau_{xy}}{G},\ \varepsilon_{xz} = \frac{\tau_{xz}}{G},\ \varepsilon_{xz} = \frac{\tau_{yz}}{G},$$

where ΔT - the difference between the temperature of a test point and the initial temperature.

Longitudinal and transverse modules of elasticity depend on the temperature, so

$$E = E(T),\ G = G(T) \quad (13)$$

In the case of elastic-plastic stress-strain state the expression (11) takes the form [23,24]

$$\sigma_i = E \cdot (1 - \omega) \cdot \varepsilon_i \quad (14)$$

where $\omega = f(\varepsilon_i)$ - the function of plasticity, which depend on the intensity of deformation.

The graphs, which are shown in Fig.6, let us to form a view about determining the function of plasticity with using the diagram of deforming of the material. The broken line, which consists the two straight lines and characterizes the change in stress intensity on the intensity of deformation, is shown in the upper fragment of this figure. The curve at the down fragment of Fig.6 describes the change in the function of plasticity, depending on the intensity of deformation.

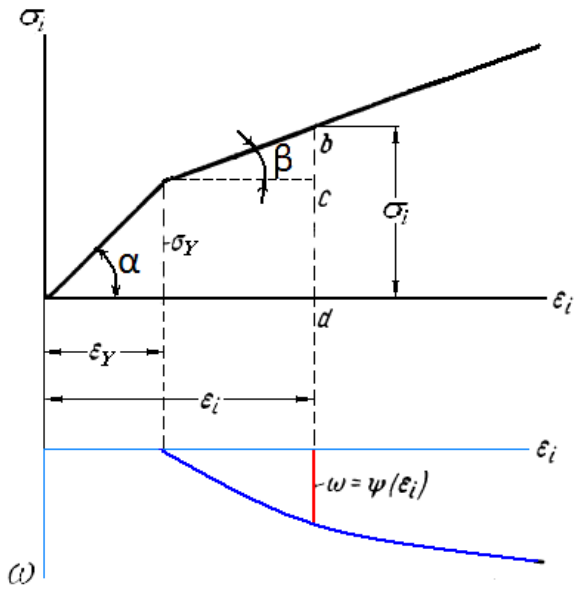

Fig.6. Determining the function of plasticity at the diagram of deforming of the material .

If the diagram of the tension-compression of the material can be represented in the form of two oblique lines, which are directed at an angle **α** and **β** to the horizontal axis, the intensity of stress at any point of the diagram can be calculated on the basis of the expression:

$$\sigma_i = E \cdot \varepsilon_i - E \cdot (\varepsilon_i - \varepsilon_Y) + E_s \cdot (\varepsilon_i - \varepsilon_Y) =$$
$$= E \cdot [1 - (1 - \frac{\varepsilon_Y}{\varepsilon_i})(1 - \frac{E_s}{E})] \cdot \varepsilon_i$$

The last relationship lets to receive an expression for the function of plasticity

$$\omega = (1 - \frac{\varepsilon_Y}{\varepsilon_i})(1 - \frac{E_s}{E}) \quad (15)$$

where ε_Y - the deformation, corresponding to the yield strength of the material; E_s - secant modulus of elasticity of the material.

For copper M1 at a temperature of 20 ° C:
modulus of elasticity E = 110 GPa,
yield strength σ_Y = 220 MPa,
secant modulus of elasticity E_s = 1,8 GPa,
coefficient of linear expansion $\alpha = 16{,}7 \cdot 10^{-6}$ 1/K.

The equations (8) - (15) describe the elastic-plastic stress-strain state of the melting tool during thermomechanical loading. To solve these differential equations it is necessary to define the boundary conditions and thus to formulate the non-linear boundary value problem. Restrictions on all displacements were imposed at the line of intersection of the bottom horizontal plane with the cylindrical surface of the melting tool.

Traditional numerical methods for calculating the stress-strain state of structures are based on the solution of nonlinear boundary value problem of elasticity theory. Discussed above, the numerical finite element method allows us to accurately take into account the geometry of the melting instrument and boundary conditions. In addition, simultaneous using of the finite element model for calculation of temperature fields and the stress state is very convenient for computation. It makes quite easy to use pre-computed temperatures at the nodes of the model for subsequent calculation of the thermal strains.

Two fragments and epure, which are depicted in Fig.7, characterize the distribution of vertical displacements in the melting tool under the analyzed thermomechanical loading. In order to ease the analysis of the mosaic of displacements, in both fragments in Fig.7 is not shown the half of niche and the adjacent bottom part of the melting tool. Analysis of the epure, which characterizes the change of the vertical displacement along the diameter of the upper surface of the niche, lets to conclude, that the bottom part of the niche is subjected by the clearly expressed bending. Areas of largest displacements are located at the left board of the niche, in the zone of maximum temperatures, and in the center of the upper surface of the niche. The maximum value of the vertical displacement is equal to 1.344 mm and is observed in the central part of the upper surface of the bottom of the melting tool.

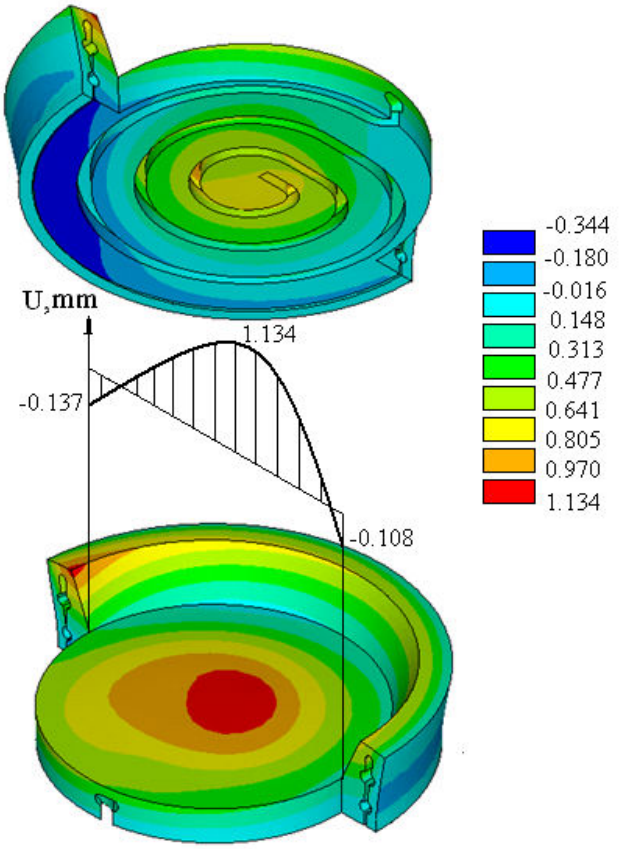

Fig.7 Mosaic of vertical displacements in the melting tool, mm

A mosaic of equivalent stresses in the design of the melting tool is shown in Fig.8. Fig.8 contains two pieces, which allow to create the most complete picture of the distribution of the equivalent stresses von Mises . Half of the melting tool, which includes the niche, is shown on the upper fragment of this figure. A similar form of the design of the melting tool, which includes the channels of the cooling system, is shown in the lower fragment.

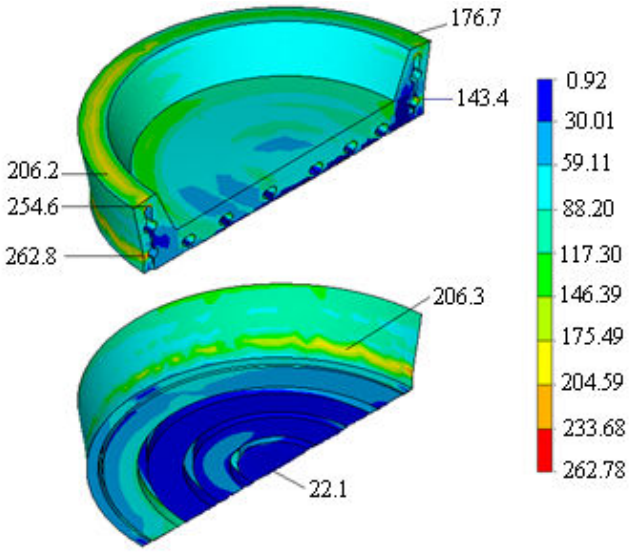

Fig.8 Mosaic of Mises equivalent stress, MPa

The color scale, which contains bands of identical values of stresses, is shown on the right side of this figure. It is seen, that the region of the greatest stress is located on the outer cylindrical surface of the melting tool, its maximum value is equal to 262,8 MPa. This value is slightly greater than the yield strength of refined copper M1, from which is made the melting tool. Temperature gradients are much less in the bottom part of the structure in comparison to other parts of the melting tool. It is because of bottom part is the subject to the most intensive cooling. So, values of stresses in this part of the structure are much less and their maximum value doesn't exceed 30 MPa.

YII CALCULATION OF THE MELTING TOOL'S RESOURCE

If the cyclic stresses exceed the yield strength of the material, the loss of design's efficiency due to the loss of strength can occur in case, when the number of cycles of the loading does not exceed one thousand. Such destruction is typical for structures, that undergo the action of the periodic loading and unloading, it is called the low-cycle fatigue. A distinctive feature of the low-cycle fatigue is that small stress increment is accompanied by a large strain increment. At the same time the providing of the design's strength under the static loading is prerequisite. Analysis of low-cycle fatigue is associated with the decision of the two main tasks:

1. It is necessary to figure out an equation for calculating the mechanical states of elasto-plastic deformation with taking into account the cyclical volatility of the material and one-sided accumulation of plastic deformations. This equation should not require an excessive amount of preliminary laboratory studies to determine the required material parameters;
2. It is necessary to construct a kinetic equation of damage under cyclic fatigue, which is associated with the appearance of loops of the plastic hysteresis.

With regard to the calculation of a melting tool's resource, the theory of low-cycle fatigue lets to take into account the effect of cycles of the heat loading on the growth of plastic deformation up to the formation of cracks. The strain life criterion is typically used in low-cycle fatigue for analysis of the material fatigue due to the thermal cycles of the structure. According to this criterion, the stress level may be higher and the number of cycles to failure may be lower.The Manson-Coffin Strain Life algorithm was provided for predicting uniaxial strain life [25,26]. The basic relationship of this algorithm can be written as:

$$e_{ia} = \frac{0{,}5 \cdot D^{0,6}}{N^{0,6}} + \frac{1{,}75 \cdot \sigma_{UTS}}{E \cdot N^{0,12}}$$

where

e_{ia} - peak value of the intensity of deformation,

N - the number of load cycles to failure,

D - the coefficient of ductility,

σ_{UTS} - the tensile strength of the material.

The coefficient of plasticity depends on the mechanical properties of the material and is determined on the basis of the

ratio

$$D \cong ln\frac{A_0}{A_{fra}} = ln\frac{1}{1-\psi}$$

where

A_0 - the initial cross-sectional area of the specimen,

$A_{f\,ra}$- the measured cross-sectional area at fracture,

ψ- the reduction in cross-sectional area of the specimen.

The labeled above mechanical properties of copper M1 were obtained by experiment, their values are equal:

E= 110 GPa, σ_{UTS} =265 MPa, ψ = 0,6; D = 0,916.

The curve of low-cycle fatigue of copper M1 is shown in Fig.9.

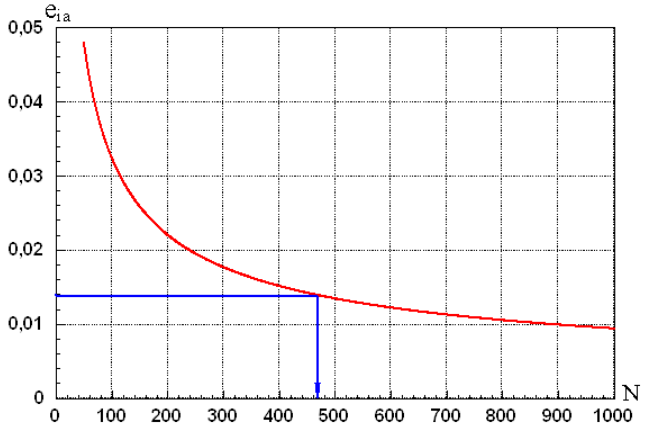

Fig.9 The curve of low-cycle fatigue of copper M1

Analysis of the calculation results of the stress-strain state of the melting tool allowed us to determine the amplitude of the intensity of deformation under the cyclic thermomechanical loading. Its value is equal e_{ia} = 1,4%. This allowed us to define the number of the cycle of thermomechanical loading with the using of the curve of low-cycle fatigue. It it necessary to hold a horizontal line through a point on the vertical axis, which corresponds to the e_{ia} = 1.4%, to the intersection with the curve, and then from the point of intersection it is necessary to hold the normal to the horizontal axis. As a result of the calculations was obtained the nuber of thermomechanical loading cycles is N = 468.

VIII Conclusion

Coupled problem of mathematical physics had been solved for a reliable assessment of the stress-strain state of the melting tool. The overall solution assumes the preliminary solution of heat conduction problem for the calculation of temperature fields and the subsequent solution of boundary value problem of elasticity theory to calculate the stresses and strains.

Using of numerical finite element method for the solution this complex problem made it possible to:

1. Take into account the real geometry of the melting tool;
2. Get the temperature field in the design of the instrument;
3. Get the field distribution of stresses and displacements in the construction of the instrument;
4. Identify areas of maximum stress;
5. Draw conclusions about of sufficient structural strength.

Acknowledgment

The analyzed variant of the melting instrument passed the technical expertise and became patented in the Russian Federation [27]. Operation of the melting tool in the corporation "VSMPO-AVISMA Corporation" for a long period of time confirmed the reliability of the proposed construction.

References

[1] Manson S., *Thermal stress and low cycle fatigue.* Moscow: Mashinostroenie,1974. – 344p.

[2] J. Sjöström, J. Bergström.Thermal fatigue in hot-working tools// *Scandinavian Journal of Metallurgy*,Volume 34, Issue 4, P. 221–231, August, 2005

[3] Gusenkov A.P. *The strength under the isothermal and nonisothermal low-cycle loading*. - Moscow: Nauka, 1979. – 296p.

[4] H-J Christ, A Jung, H J Majer and R Teteruk. Thermomechanical fatigue damage mechanisms and mechanism-based life prediction methods. *Sadhana* Vol. 28, Parts 1 & 2, February/April 2003, pp. 147–165.

[5] Mall, S., Nicholas, T., Pernot, J.J. Crack growth rate behavior of titanium-aluminide alloy during isothermal and nonisothermal conditions. *Journal of Engineering Materials and Technology*, P. 137–146,1995.

[6] Bakish R. Electron beam processing refines metall purity, *Advanced Mater*, №12, 1992,pp. 25-32

[7] Paton B.E, Trigub N.P, Ahonin S.V, Zhuk G.V.*Electron-beam melting of titanium.* Kiev, Naukova Dumka, 2006.

[8] A.V.Lykov. *Heat and Mass Transfer (Handbook)*. Moscow: Energiya, 1978.

[9] H.Y.Wong. *Handbook of Essential Formulae and Data on Heat Transfer for Engineers*, Longman Group United Kingdom ,1977.

[10] Y. Jaluria, Numerical Study of the Thermal Processes in a Furnace, *Numer. Heat Transfer*,7, 1984, pp. 211–224.

[11] Syakila Ahmad, Norihan Md. Arifin, Roslinda Nazar, Ioan Pop. Mathematical Modeling of Boundary Layer Flow Over a Moving Thin Needle With Variable Heat Flux. *Proceedings of the 12th WSEAS Int. Conf. on APPLIED MATHEMATICS, Cairo, Egypt*, 2007, pp.48-54

[12] Fernando Carapau, Adelia Sequeira. Axisymmetric flow of a generalized Newtonian fluid in a straight pipe using a director theory approach.*Proceedings of the 8th WSEAS Int. Conf. on APPLIED MATHEMATICS, Tenerife, Spain*, 2005, pp.303-308

[13] Bellot J. P., Jardy A., Ablitzer D.Modelisation du comportement thermique d'un lingot de titane refondu par bombarderaent electronique, *Rev. de Metallurgie.* № 5, 1993, pp. 675-683.

[14] M. Blum, A. Choudhury, F. Hugoetal. Results of electron beam remelting of superalloys and titanium alloys with a high-frequency EB-gun , *Ibid.* - 1993, pp. 102-115.

[15] R. V. Goldstein N. M. Osipenko. Modeling of coating separation under thermomechanical loading in the beam approximation. Mech. Solids. 42 (5), 2007, pp.723-736

[16] K.A. Goncharov. Stress-strain state and safe life of the crucible of a skull furnace under thermomechanical loading. *Metallurgist:* Vol. 54, Issue 11, 2010, pp.852-858.

[17] Konstantin A. Goncharov, Yuri B. Chechulin. Stress state of a tool for stamping tubes. *Journal of International Scientific Publications*: *Materials, Methods and Technologies,* V.5/1, 2011, pp.212-221.

[18] Konstantin A. Goncharov, Yuri B. Chechulin. Stress-strain state of mill for cold rolling of tubes. *Journal of International Scientific Publications*: *Materials, Methods and Technologies*, V.5/1, 2011, pp. 222-229.

[19] A.V. Zabolotsky. Computer simulation of thermal shock in refractory linings of metallurgical installations. *International Journal of Mathematical Models and Methods in Applied Sciences*, Issue 3, Volume 5, 2011, pp. 73-76.

[20] Coman Gelu, Krisztina Uzuneanu, Tanase Panait, Maricel Dragan.Use of the Finite Element Method in Modelling the Heat Transfer inside an Artificial Skating Rink. *Proceedings of the 9th IASME / WSEAS Int. Conf. on HEAT TRANSFER, THERMAL ENGINEERING and ENVIRONMENT (HTE '11),* Florence, Italy, pp. 277-282.

[21] B. A.Kermani. Numerical investigation of heat transfer process form exothermic board by natural convection inside a closed cavity. *Proceedings of the 8th IASME / WSEAS Int. Conf. on HEAT TRANSFER, THERMAL ENGINEERING and ENVIRONMENT (HTE '10).* Taipei, Taiwan, 2010*,* pp.163-168

[22] Richard B. Hetnarski, Jozef Ignaczak. *Mathematical theory of elasticity.* Taylor & Francis, 2004.

[23] A.A.Ilyushin. *Plasticity. Part one. Elastic-plastic deformation*. Moscow, 2004.

[24] R. Hill, *The Mathematical Theory of Plasticity*, Oxford University Press 1998.

[25] Manson, S. S. Behavior of Materials under Conditions of Thermal Stress. *Heat Transfer Symposium, University of Michigan Engineering Research Institute*, 1953

[26] V.M. Radhakrishnan. On the bilinearity of the Coffin-Manson low-cycle fatigue relationship. *Metallurgical Engineering Department, Indian Institute of Technology,* Madra 600 036, India

[27] Altman P.S, Fomichev V.S, Goncharov K.A. *Pat. № 2226222 Russian Federation.Melting tool.* IPC C22B9/21,F27B14/08.Publ.27.03.2004.